Epidemiol. Infect. (2000), **124**, 529–541. Printed in the United Kingdom

EPIFIL: The development of an age-structured model for describing the transmission dynamics and control of lymphatic filariasis

R. A. NORMAN[1,2]*, M. S. CHAN[2], A. SRIVIDYA[3], S. P. PANI[3], K. D. RAMAIAH[3], P. VANAMAIL[3], E. MICHAEL[2], P. K. DAS[3] AND D. A. P. BUNDY[2]

[1] *Department of Computing Science and Mathematics, University of Stirling, Stirling FK9 4LA, UK*
[2] *Wellcome Trust Centre for the Epidemiology of Infectious Disease, Department of Zoology, University of Oxford, South Parks Road, Oxford OX1 3PS, UK*
[3] *Vector Control Research Centre, Medical Complex, Indira Nagar, Pondicherry-605 006, India*

(*Accepted 3 February 2000*)

SUMMARY

Mathematical models of transmission dynamics of infectious diseases provide a useful tool for investigating the impact of community based control measures. Previously, we used a dynamic (constant force-of-infection) model for lymphatic filariasis to describe observed patterns of infection and disease in endemic communities. In this paper, we expand the model to examine the effects of control options against filariasis by incorporating the impact of age structure of the human community and by addressing explicitly the dynamics of parasite transmission from and to the vector population. This model is tested using data for *Wuchereria bancrofti* transmitted by *Culex quinquefasciatus* in Pondicherry, South India. The results show that chemotherapy has a larger short-term impact than vector control but that the effects of vector control can last beyond the treatment period. In addition we compare rates of recrudescence for drugs with different macrofilaricidal effects.

INTRODUCTION

Lymphatic filariasis is a mosquito-borne parasitic infection that occurs in many parts of the developing world [1, 2]. The symptoms and disability caused by this infection have a high social and economic impact on infected individuals [3, 4]. This, together with the considerable recent advances made in developing intervention tools [5], has led to renewed global interest in controlling or even eliminating this infectious disease [6]. Currently the two main ways of controlling the disease are vector control and mass chemotherapy.

Mathematical modelling of parasite transmission dynamics has proved to be a useful aid to exploring the probable outcome of community level control programmes [7]. Simple mathematical models of infection have been in existence for filariasis since the 1960s [8–10]. These have provided useful insights into the dynamics of infection and disease in human populations [11–14], but have been less helpful in assessing the impact of community-targeted control options for two main reasons. They do not explicitly take account of the age structure of the human population or of the transmission dynamics of infection to and from the vector population. However, both of these factors are thought to be important [14–16].

In addition to these simple models a stochastic micro-simulation model of lymphatic filariasis, LYMFASIM, has been developed [17]. Whilst this model is much more biologically realistic and hence of more practical use than the simple models it still does not

* Author for correspondence.

explicitly include the dynamics of infection within the vector population.

Recently, we developed and parameterized a constant force-of-infection cohort model [18]. In this paper, we extend the basic structure of this model by incorporating explicitly both host age structure and vector transmission dynamics in order to provide a more realistic framework for assessing the consequences of the different intervention options currently available for filariasis control. The model includes age-dependent functions of infection as well as the effects of the demographic age structure of the human community. The latter is of particular importance for filariasis because of the long lifespan of the worm.

The model is validated with data from a vector control programme in Pondicherry, South India, an area endemic for Bancroftian filariasis transmitted by the mosquito species *Culex quinquefasciatus*.

CONCEPTUAL FRAMEWORK

The model described in this paper is developed from a cohort model described previously [18]. We extend this model to incorporate the whole transmission cycle, including the mosquito vector population. This results in a fully age structured model which is described by partial differential equations. This type of framework was first developed for helminth infections by Anderson and May [19] and has been successfully developed and validated for schistosomiasis [20].

The current model is conceptually similar to the schistosomiasis model with the important difference of the inclusion of the insect vector population. In this model, we treat the mosquito population as being of a constant size, this being defined in terms of the mean biting rate per person per month. The dynamics of infection in the vectors provide a density dependent mechanism whereby there is a limitation on the number of L3 larvae that can develop in a mosquito.

The distribution of infection between hosts of different ages in lymphatic filariasis differs markedly from schistosomiasis. Whereas schistosomiasis infection is generally most intense in children, the reverse is true of lymphatic filariasis. This is reflected in a different force of infection function; we assume here, that the biting rate increases linearly until the age of 9 years after which it is constant throughout adulthood [18]. This reflects both behavioural differences and available skin area.

Our previous paper demonstrated that the observed distribution of infection intensity with age was consistent with the action of acquired immunity [18]. This mechanism is included in the model where it is assumed that past experience of infection results in a reduction in the rate of establishment of new infections. In the previous paper there was no statistical evidence for the decay of acquired immunity and therefore acquired immunity is assumed lifelong in the current model.

Model inputs and outputs were chosen to reflect the availability of field data, in particular those available at the field site in Pondicherry. Input to the model is the biting rate of mosquitoes and the community microfilarial load. Output is the age specific prevalence and intensity of infection. Prevalence is estimated from intensity using the negative binomial distribution in the following way. The prevalence of infection at age a, $p(M(a))$ is given by

$$p(M(a)) = 1-(1+M(a)/k)^{-k}, \quad (1)$$

where $M(a)$ is the mean intensity at age a and k is inversely related to the aggregation of the parasite within the host.

We investigate the behaviour of the model in response to vector control and chemotherapy. Vector control is modelled as a percentage reduction in the vector biting rate over a specified time interval. Mass chemotherapy (targeted at all age groups) is assumed to involve an instantaneous reduction in the number of microfilariae and adult worms at the time of treatment and a cessation of microfilarial production over a specified interval. The relative proportions of the macro- and micro-filaricidal effects can be varied.

MODEL DEVELOPMENT

The model is a system of partial differential equations describing the patterns of infection over age and time. We consider two state variables reflecting the infection status of the human host, the mean worm burden and the mean microfilarial count (measured as mf per 20 μl of blood) as well as the mean acquired immunity level (in worm-years). These are all age dependent. The infection status of vectors is described by the mean number of infective L3 larvae per mosquito, which is not age dependent (and therefore described by an ordinary differential equation). The differential equations describing the rates of change of the four variables, mean worm burden (W), mean microfilarial

count (M), mean acquired immunity level (I) and mean number of L3 per mosquito (L) are given below:

$$\frac{\partial W}{\partial t}+\frac{\partial W}{\partial a}=\lambda\frac{V}{H}\psi_1\psi_2 s_2 h(a)L^* \mathrm{e}^{-\beta I}-\mu W, \quad (2)$$

$$\frac{\partial M}{\partial t}+\frac{\partial M}{\partial a}=\alpha W-\gamma M, \quad (3)$$

$$\frac{\partial I}{\partial t}+\frac{\partial I}{\partial a}=W, \quad (4)$$

$$\frac{\mathrm{d}L}{\mathrm{d}t}=\lambda\kappa g\int_a \pi(a)(1-f(M))\mathrm{d}a-\sigma_1 L-\lambda\psi_1 L. \quad (5)$$

Here $\lambda(V/H)$ is the number of bites a host receives per unit time where λ is the number of bites per mosquito per unit time, V is the number of vectors and H is the number of hosts; ψ_1 is the proportion of L3 which leave the mosquito when it bites; ψ_2 is the proportion of those L3 leaving the mosquito which enter the host and s_2 is the proportion of those L3 entering the host which survive to become adult worms. The rate at which individuals of age a are bitten is proportional to $h(a)$, this function exhibits a linear increase up to the age of 9 years and then becomes unity. L^* is the equilibrium density of L3 larvae (see later). The parameter μ is the death rate of adult worms and β is a measure of the strength of acquired immunity. The acquired immunity increases with worm burden.

For microfilariae, α is the production rate of microfilariae per worm and γ is the death rate of microfilariae. The acquired immunity level is assumed to be equivalent to the accumulated worm burden, that is the experience of infection.

In the equation for L3 [eqn (5)], λ is the number of bites per mosquito per unit time; g is the proportion of bites which are made on infected people and which result in the mosquito becoming infected; $\pi(a)$ is the age distribution of the population under consideration (Fig. 1); σ_1 is the death rate of L3s and ψ_1 is the proportion of L3 which leave the mosquito when it bites.

Since L changes more rapidly than the other variables we assume that it instantaneously adjusts to equilibrium. Therefore, the model can be simplified by deriving an expression for this equilibrium. Studies of parasite dynamics in vectors have suggested that the relationship between the number of larvae developing in the vector and the number ingested can take one of three forms, namely facilitation, limitation or proportionality and that these patterns have major implications for the overall population dynamics [16, 21]. For the species under consideration in this study, *Wuchereria bancrofti* transmitted by *Culex quinquefasciatus*, limitation is the most appropriate model [16] and we use the following function to describe the number of infective L3 larvae developing from an infective host with microfilaria count of M.

$$L=\kappa(1-\mathrm{e}^{-rM/\kappa}), \quad (6)$$

where r and κ are constants which were estimated from data in [22]. This is a logistic growth function where κ is the saturation level and r a measure of the initial increase in L3 larvae uptake as M increases from 0.

To derive an expression for L^* the equilibrium number of L3 larvae per mosquito, we need to solve $\mathrm{d}L/\mathrm{d}t=0$. Using equation (4) we obtain

$$L^*=\frac{\lambda\kappa g\int_a \pi(a)(1-f(M))\mathrm{d}a}{\sigma_1+\lambda\psi_1}, \quad (7)$$

which can then be used in equation (1).

The function $f(M)$

$$f(M)=\left(1+\frac{M}{k(M)}(1-\mathrm{e}^{-r/\kappa})\right)^{-k(M)} \quad (8)$$

is the population effect of the limitation mechanism in mosquitoes. It comes from combining the rate of uptake of infection by mosquitoes [eqn (6)] with the assumed negative binomial distribution [eqn (1)].

The model is run by assuming that the population parasite distribution is initially at equilibrium. This equilibrium is calculated for a given situation by using the observed monthly biting rate and community mf load, and then fitting the survival of L3 larvae (s_2) as a free parameter. Treatment by chemotherapy or vector control perturbs this equilibrium.

A computer program to implement this model was written in FORTRAN. The differential equations were solved using a numerical finite difference method (Euler type method).

MODEL VALIDATION

The model was tested against data from an integrated vector management (IVM) control programme implemented between 1981–5 in Pondicherry (12° N, 80° E), South India [23, 24].

Data on human infection involved three population surveys in 1981, 1986 and 1989 where 20 μl blood smears were taken from an age stratified 5% sample of the population [23–25]. Entomological measurements were taken continuously throughout this period; resting and biting densities were determined

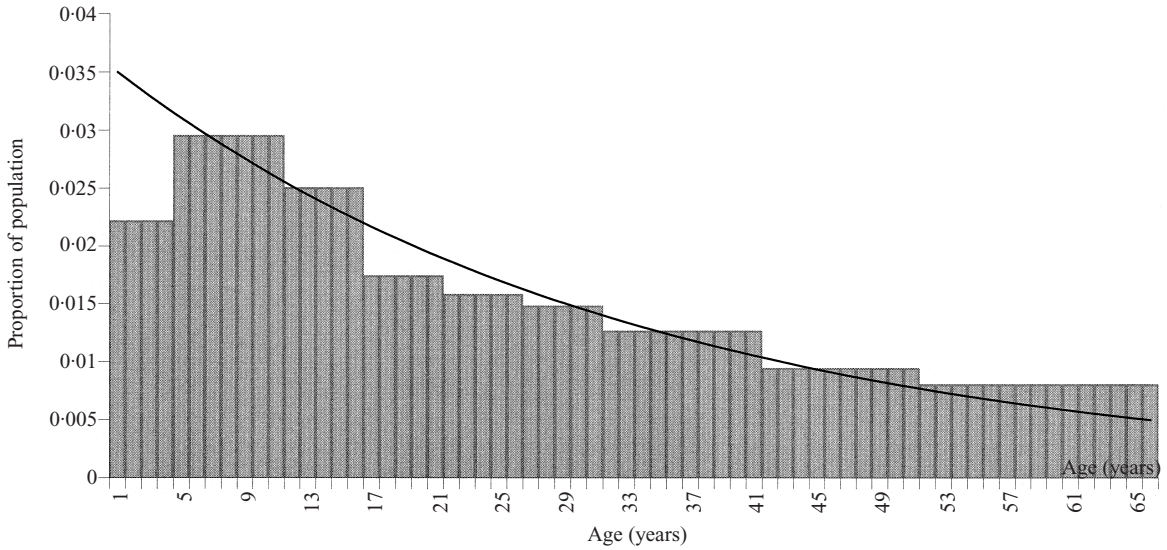

Fig. 1. Population age distribution data for Pondicherry (bars) and the age distribution used in the model (line).

Table 1. *Default values for parameters*

Symbol	Meaning	Value (per month)	Source
λ	Number of bites per mosquito	10	[35–37]
κ	From uptake of L_3 relationship	6	Estimated from [22]
r	From uptake of L_3 relationship	0·047	Estimated from [22]
g	Proportion of mosquitoes which pick up infection when biting an infected host	0·37	Estimated from [22]
σ_1	Death rate of mosquitoes	5	[38]
ψ_1	Proportion of L_3 leaving mosquito per bite	0·414	[9]
ψ_2	Proportion of those L_3 leaving mosquito which enter host	0·32	[38]
$k(M)$	Aggregation parameter from negative binomial distribution	$0{\cdot}0029 + 0{\cdot}0236 \times M$	Estimated from data [23, 24]
β	Strength of acquired immunity	0·112	Estimated by model
μ	Death rate of adult worms	0·0104	[3, 39–41]
$\lambda(V/H)$	Rate at which humans are bitten	Initially 5760	[23, 24]
s_2	Proportion of L_3 entering host which develop into adult worms	$1{\cdot}13 \times 10^{-4}$	Estimated by model
α	Production rate of microfilaria per worm	2	[42]
γ	Death rate of microfilaria	0·1	[39, 42]

Table 2. *Vector biting rate in control areas from* [*23*, *24*]

Year	1980	1981	1982	1983	1984	1985	1986	1987	1988	1989
Biting rate (per month)	5760	576	384	192	192	384	1152	1536	2880	1536

every 2 weeks at a site in the IVM area. These measurements were continued after the cessation of IVM.

Parameters for the model validation are reported in Table 1, with sources. To validate the model, free parameter s_2 was fitted to the initial age prevalence profile using maximum likelihood assuming binomial errors. The model was then run using the observed values for reductions in vector biting rate (Table 2) and compared with the data at the end of the control programme in 1986 and 1989 (Figs. 2–4).

The fit of the model was estimated as the deviance

Table 3. *Statistical comparison of data with model output and percentage of variation, R^2, in the prevalence data explained by the model*

Year	χ^2	D.F.	P	R^2
1981	21·3354	10	0·019	93·1%
1986	82·8471	10	0·000	73·2%
1989	172·457	9	0·000	71·5%

(twice the log-likelihood ratio) which is distributed as χ^2 and is calculated in the following way:

H_0: prevalence estimated by model has the same distribution as the data;

H_1: prevalence estimated by the model has a different distribution to the data.

Let p_{im} be the prevalence in age class i estimated by the model and p_{id} be the actual prevalence in age class i (the data, $i = 1, \ldots, n$). If N is the sample size in each age class and r is the number infected in each age class and we assume infection is binomially distributed then the log likelihood ratio is

$$-2\ln\left(\frac{\binom{N}{r}(p_{im})^r(1-p_{im})^{N-r}}{\binom{N}{r}(p_{id})^r(1-p_{id})^{N-r}}\right)$$
$$= -2(r\ln(p_{im}) + (N-r)\ln(1-p_{im}) - r\ln(p_{id}) - (N-r)\ln(p_{id})),$$

this is summed over all age groups and the answer compared to a χ^2 distribution with $n-2$ degrees of freedom.

We also calculated the proportion of the variation explained by the model, this is equivalent to the coefficient of determination R^2 and is calculated using the following equation:

$$R^2 = 1 - \frac{\Sigma(p_i - \hat{p}_i)^2}{\Sigma(p_i - \bar{p})^2} \quad (9)$$

where p_i is the prevalence observed in age class i, $\hat{p}_i$ is the model prevalence for age class i and $\bar{p}$ is the average prevalence in the year (Table 3).

SIMULATION OF TREATMENT PROGRAMMES

The model was used to investigate and compare the long-term impact of two different control strategies: IVM and single-dose mass chemotherapy.

The aim of IVM is to reduce the number and hence the biting rate of mosquitoes, which should result in a decrease in infection rates and ultimately, disease. In Pondicherry, vector control was achieved by reducing the number of sites available for mosquito larval development [24, 25]. The vector control simulation described here (Simulation 1) was based on the reductions in biting rate observed in Pondicherry.

Table 4. *Microfilaria intensity data for 1989 including upper confidence limit*

Age	Mean mf intensity	Upper 95% confidence limit
0–5	0·06	3·19
6–8	0·22	3·07
9–11	0·56	3·28
12–14	0·57	2·87
15–19	0·77	3·13
20–24	0·83	3·04
25–29	0·81	3·18
30–34	0·6	3·09
35–44	0·61	2·93
45–54	0·58	3·00
$\geqslant 55$	0·93	3·38

The chemotherapy programmes simulated here (Simulations 2–4) are based on recommended procedures rather than an actual programme. We consider chemotherapy with the two most common anti-filarial drugs, DEC (diethylcarbamazine citrate) and ivermectin. WHO currently recommends that treatment programmes should be based on yearly mass treatment with a single dose regimen and this is the type of programme simulated here.

It is thought that the two drugs have different efficacies. Treatment with either drug results in rapid clearance of microfilariae followed by a period in which microfilariae are not produced. Ivermectin has a somewhat higher efficacy in this regard. However, it is thought that ivermectin kills very few adult worms whereas DEC kills a significant proportion of adult worms. We simulate three different chemotherapy programmes based on estimated efficacies of the two drugs. In all the cases, chemotherapy occurs yearly for the first 5 years and the simulation is run for 10 years.

The following four simulations were carried out.

Simulation 1. Vector control for 5 years with a reduction in biting rate of 94% followed by a period of 5 years with no active vector control where biting rates are still 70% lower than before the programme, presumably because of residual benefits from reducing breeding sites [24].

Simulation 2. Chemotherapy with DEC with 80%

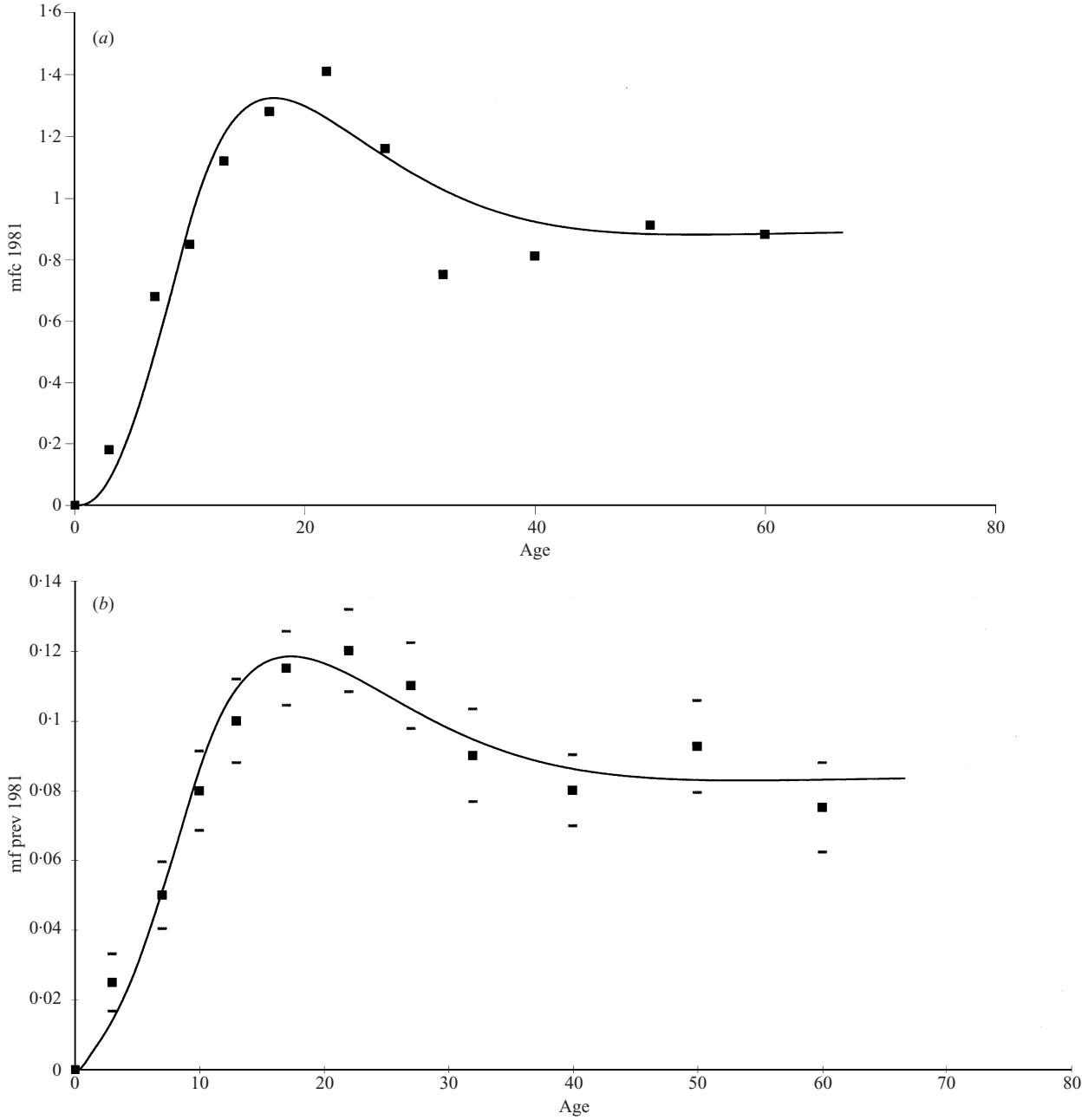

Fig. 2. Graphs of (*a*) Microfilaria age intensity (mfc) distribution in Pondicherry in 1981. (*b*) Microfilaria age prevalence (mf prev) distribution in Pondicherry in 1981. In each case the curve represents the model output and the squares represent the data. In the case of the prevalence graph we have also included the 95% confidence limits.

coverage; 40% of adult worms are assumed killed and 95% of microfilariae, with no more microfilariae being produced for 6 months after treatment.

Simulation 3. Chemotherapy with ivermectin with 80% coverage; 10% of adult worms are killed and 99% of microfilariae, with no more microfilariae being produced for 3 months after treatment.

Simulation 4. Chemotherapy with DEC and ivermectin with 80% coverage; 50% of adult worms are killed and 99% of microfilariae, with no more microfilariae being produced for 6 months. Note that the combined effect assumes that the drugs are given sequentially so that, as a first estimate, the macrofilaricidal effects are additive [26]. However we also assume that 99% is the maximum possible microfilaricidal effect.

The results of the simulations are shown in three dimensional surface plots with mean mf count on the

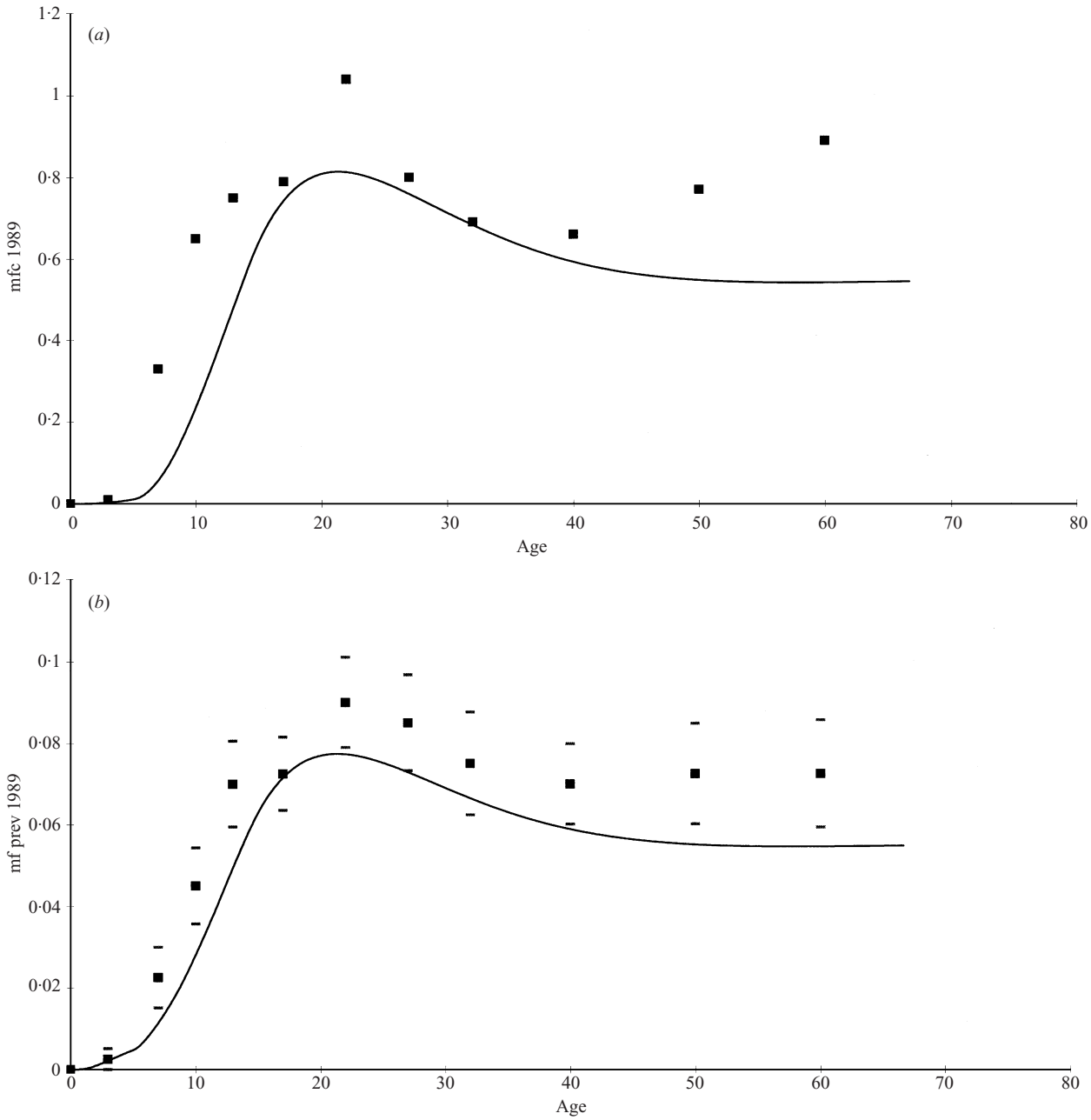

Fig. 3. Graphs of (*a*) Microfilaria age intensity distribution in Pondicherry in 1986. (*b*) Microfilaria age prevalence distribution in Pondicherry in 1986. In each case the curve represents the model output and the squares represent the data. In the case of the prevalence graph we have also included the 95% confidence limits.

vertical axis and age and time on the horizontal axes (Figs 5–8). They are also illustrated as overall changes in mf count by year (Fig. 9).

RESULTS

Model validation

The statistical analysis of the model validation using age-prevalence data is shown in Table 3. This includes the calculation of deviances and the proportion of the variability explained by the model. For the intensity data, which were very variable, the means and upper 95% confidence limits for 1989 are shown in Table 4 for illustrative purposes. The lower confidence limits were close to zero in all cases.

For the baseline data (fitted to model), the model describes adequately the initial age prevalence curve (Fig. 2*b*), explaining 93·1% of the variability (Table 3). The age intensity curve (Fig. 2*a*) is also well described by the model. In addition, if we compare the

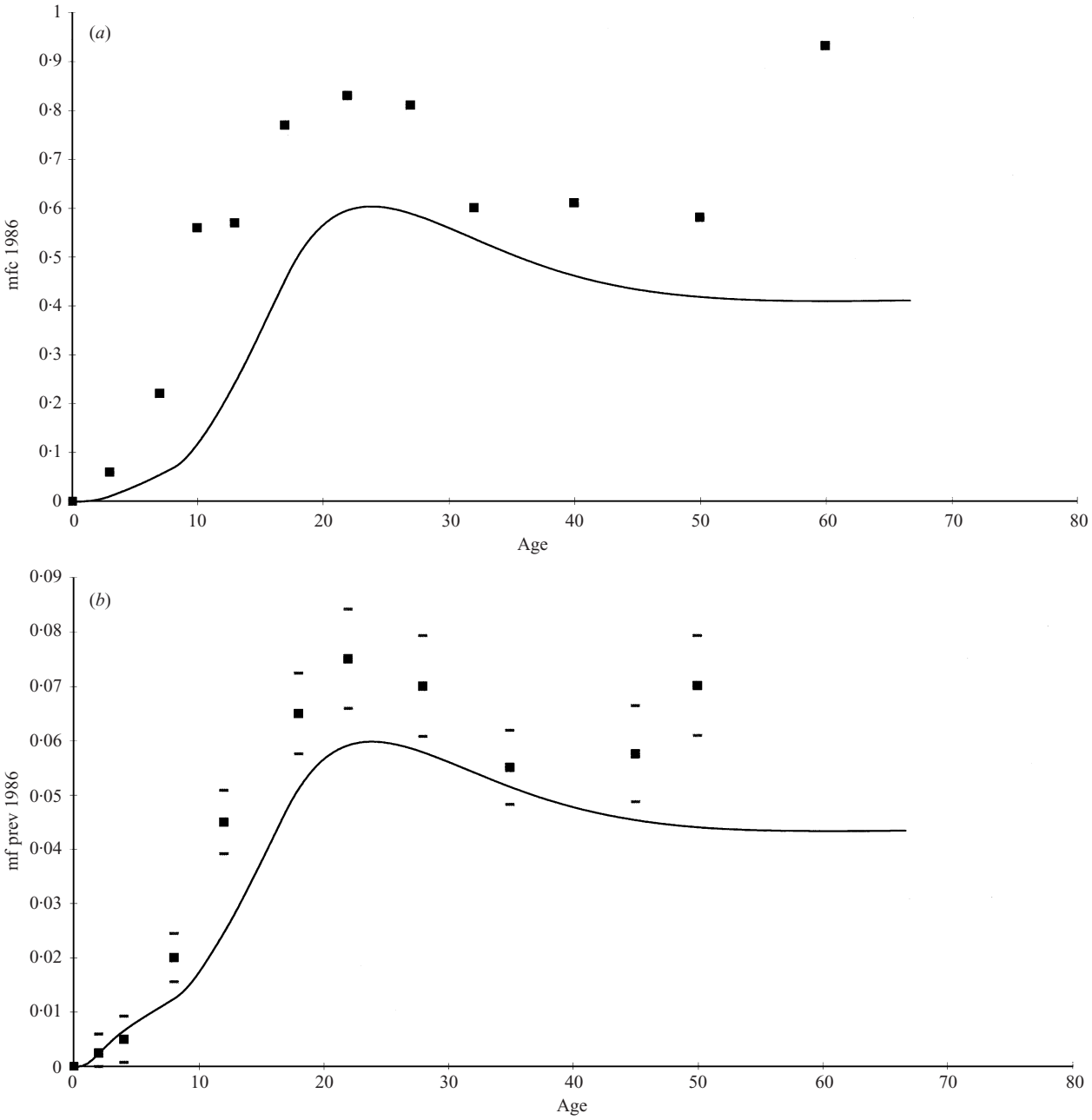

Fig. 4. Graphs of (*a*) Microfilaria age intensity distribution in Pondicherry in 1989. (*b*) Microfilaria age prevalence distribution in Pondicherry in 1989. In each case the curve represents the model output and the squares represent the data. In the case of the prevalence graph we have also included the 95% confidence limits.

predicted equilibrium number of L3 larvae per mosquito (0·014) with the observed value (0·03 [27]) then we can conclude that overall the model describes the data reasonably well.

For the 1986 simulation, the model explains 73·2% of the variability in the observed data and shows a similar trend, but differs significantly (Table 3) from the observed data ($P < 0{\cdot}01$). Examination of the graphs of intensity (Fig. 3*a*) and prevalence (Fig. 3*b*) shows that both are underestimated. The underestimation is more marked in 1989, where the model explains 71·5% of the variability and the model is again statistically significantly different from the observed data (Table 3). These relationships are illustrated in Figure 4(*a*, *b*).

Simulation of treatment programmes

Figure 5 shows the results of the simulation of vector control (Simulation 1). As in the programme in

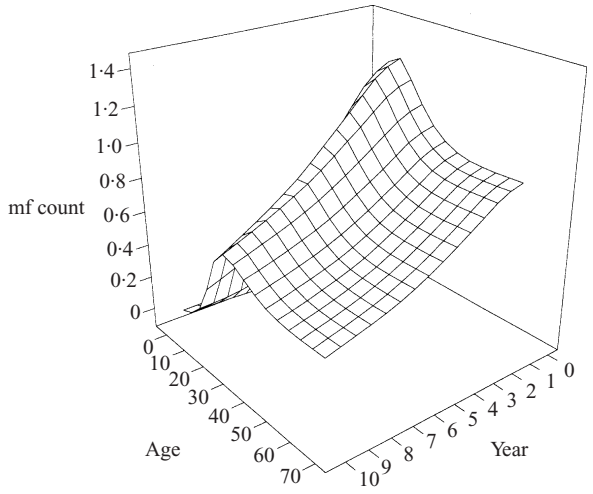

Fig. 5. Three-dimensional graph to show the microfilaria age intensity distributions predicted by the model for 10 years of vector control as described in the text.

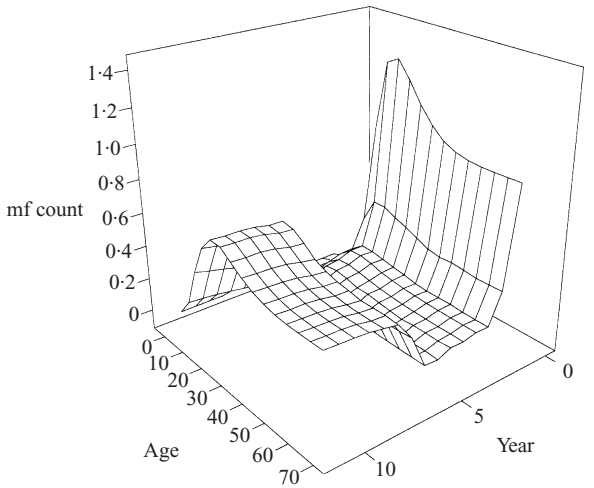

Fig. 7. Three-dimensional graph to show the microfilaria age intensity distribution predicted by the model for 5 years of treatment with ivermectin as described in the text.

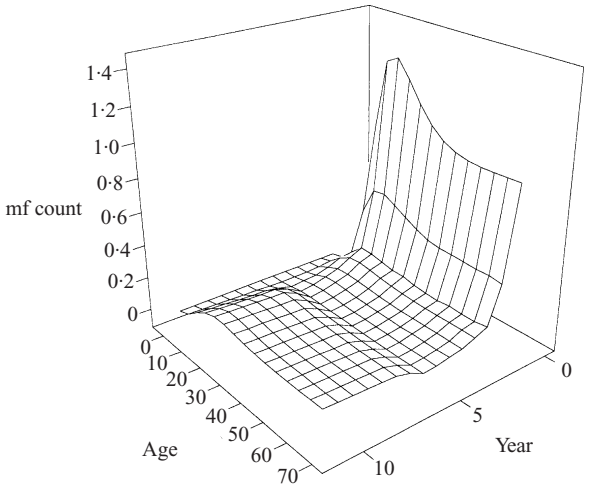

Fig. 6. Three-dimensional graph to show the microfilaria age intensity distribution predicted by the model for 5 years of treatment with DEC as described in the text.

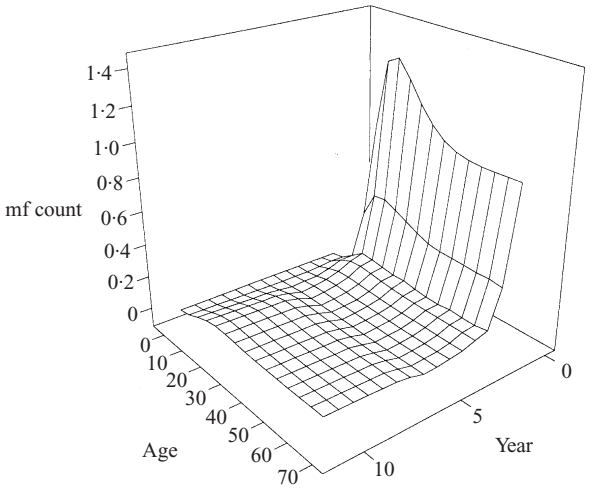

Fig. 8. Three-dimensional graph to show the microfilaria age intensity distribution predicted by the model for 5 years of treatment with a combination of DEC and ivermectin as described in the text.

Pondicherry, it is assumed that during the period of active vector management (first 5 years), there is a 94% reduction in vector biting rates. For the following 5 years, active vector management is not continued, but the structural changes made in the first 5 years mean that vector biting rates remain depressed at 70% of the pre-control level. The figure predicts a gradual decrease in human infection levels over this entire period. The average mf count (over all ages) is plotted with the results of the other simulations in Figure 9. Note that since there is no treatment in this simulation, human infection levels do not decrease immediately, but only after a time delay as the reduced biting rates lead eventually to fewer infections. In particular, the vector management control programme will avert new infections in the youngest age groups. After the cessation of active vector management, the continuing lower biting rates result in a continued decline in the levels of infections in the human population.

The population dynamic consequences of the simulated chemotherapy programmes (Figs 6–9) are very different from vector control, regardless of the drug used. There is a direct and immediate reduction in human infection levels and the treated individuals, in particular, enjoy an immediate reduction in infection intensity. In the short term, the chemo-

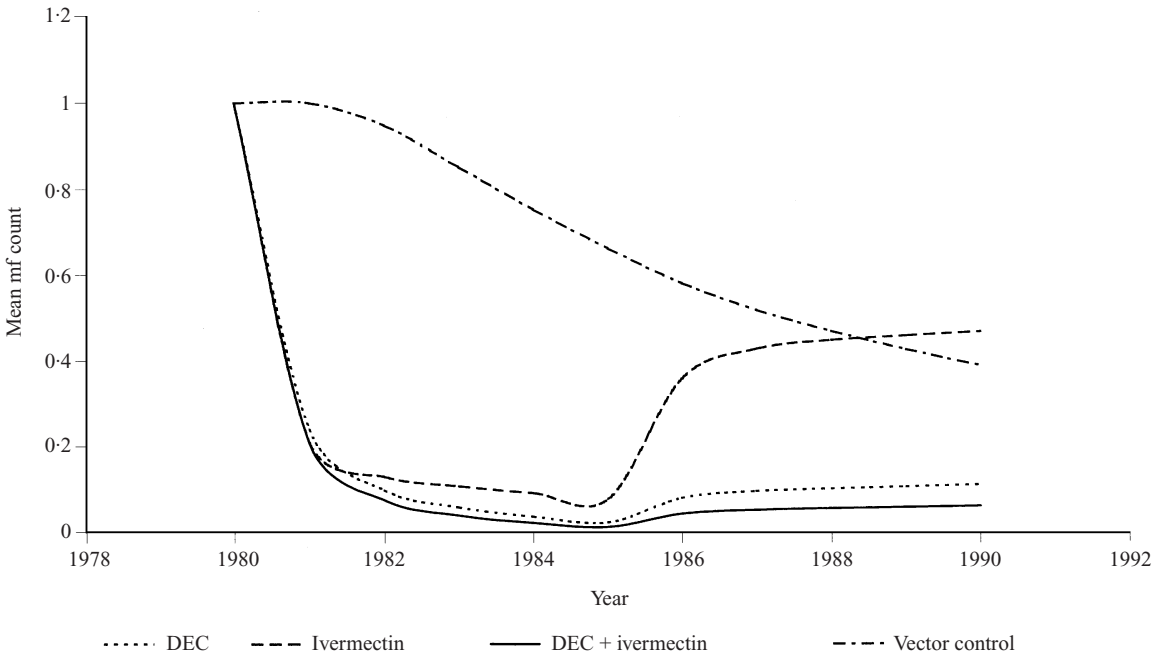

Fig. 9. Graph to show how the mean microfilaria intensity changes over the 10 years simulated by the model for the four different treatment regimens described in the text.

therapy programmes are more effective. However, a question of interest for chemotherapy programmes is the reinfection levels after the cessation of treatment. This appears to depend on the properties of the treatment, which is explored in Simulations 2–4 (Figs 6–8).

DEC alone (Simulation 2; Figs 6 and 9), which has a high efficacy against microfilariae and a moderate efficacy against adult worms, results in an initial sharp drop in infection levels followed by a sustained reduction while the treatment programme continues. When the treatments are discontinued (after year 5), reinfection occurs but at a low level.

For treatment with ivermectin alone (Simulation 3: Figs 7 and 9), which has a very high efficacy against microfilariae but almost no effect on adult worms we observe a slightly faster initial reduction in infection levels and sustained very low infection levels while the treatment programme continues. However, on cessation of treatment the pattern of reinfection is very different from DEC. Since ivermectin effectively has no impact on the adult worms, which live on average for 8 years, the worms are still present once treatment is discontinued and begin again to produce microfilariae. Therefore, there is a very rapid recovery of microfilariae levels on cessation of control. The infection level does not return immediately to pre-control levels as the period of low microfilarial intensity has led to a reduction in transmission.

The effect of the combination treatment with both DEC and ivermectin (Simulation 4) is shown in Figures 8 and 9. This shows an almost identical pattern to treatment with DEC alone. This result underlines the importance of considering the macrofilaricidal activity of the drugs when designing a chemotherapy programme as this property is particularly important in determining the recovery rate of the infection if a treatment programme has a finite life or is interrupted.

DISCUSSION

In this paper, we have attempted to develop a realistic transmission model for lymphatic filariasis by extending an earlier version of the EPIFIL model [18]. This is achieved by incorporating the age structure of the human community and the dynamics of infection within the vector population. The inclusion of host age is necessary not only to account for age-dependencies in contact with infection [7, 28] but also because the adult worms are long lived. The explicit treatment of transmission to and from the vector population is essential, on the other hand, if the model is to be used as a predictive tool to estimate the effects of control.

Here we use the model for two purposes. First, to assess its value as a tool in predicting the quantitative

outcomes of control and secondly, to examine and compare the likely qualitative outcomes of different control strategies.

When the model predictions for the effects of vector control are compared to observed data from Pondicherry it is apparent that the qualitative trends were represented appropriately but that the quantitative predictive power declined with the period of control. This could reflect changes in either local transmission environment or may reflect the impact of uncertainties in model specification. In this respect, resolution of uncertainties in three areas of the population biology of filariasis are likely to improve the quantitative predictive value of the present model.

First, this model includes acquired, life-long immunity to parasite establishment as the only major form of density dependence operating against infection in humans. Several other mechanisms, such as an immunity induced reduction in production of microfilaria and an immunopathological response may occur [12, 29, 30].

The second area of uncertainty arises because, despite recent advances in immunodiagnosis [31] and ultrasound scanning [32, 33], it is still not possible to measure worm burdens in the field. This is important in terms of the recrudescence of infection following chemotherapy.

A third problem with model specification concerns the exposure rate of individuals to infection in typical endemic communities. Here, based on indirect evidence [10] and as a first approximation, we have considered that the vector biting rate on individuals in the Pondicherry area increases linearly until the age of 9 years after which it settles to a constant value. A more recent analysis of *Cx. quinquefasciatus* biting behaviour in the same area, however, suggests that the field biting rate may change nonlinearly with the age of individuals and may exhibit significant gender differences [28].

Despite these caveats, the results demonstrate the potential of EPIFIL as an analytical tool for comparing the relative, qualitative effectiveness of the various options for controlling filariasis. The results suggest that the dynamics of control are fundamentally different between the vector and chemotherapy-based approaches. Reduction in mean worm load in the community is gradual with vector control (duration depending on the lifespan of the parasite) while the dynamics of reduction in microfilaraemia is dramatically faster with chemotherapy. For both methods, the worm population is expected to recover unless the control measures reduce infection below a threshold.

Of the three chemotherapy regimens studied (DEC, ivermectin and combined DEC and ivermectin), our analysis suggests a superiority of the DEC-based methods in reducing community microfilarial loads. Under the same compliance and treatment plans, DEC alone or in combination is predicted to depress microfilarial loads much longer than ivermectin alone, over the 10-year time period under study. This is because of the much lower macrofilaricidal effect of ivermectin. The implication of this result is that the longer term benefits of control will be crucially dependent on the period of control versus the longevity of the worm. Here we assume mean expected life span to be 8 years (see [18]), although values as low as 3·5 years have been estimated [14].

The results also suggest that there is relatively little benefit in combining ivermectin with DEC, although DEC adds considerably to the benefits of ivermectin because of the macrofilaricidal effect. This has important implications for the proposed combination of Albendazole with ivermectin for filariasis control in Africa (WHO). Since Albendazole is reportedly macrofilaricidal [34] the combination should have enhanced long-term effectiveness, even though the difference would not be apparent in the short term when the much more immediate efficacy of ivermectin would dominate.

In conclusion, we have developed a dynamic model framework for bancroftian filariasis, which may adequately describe the transmission of this parasite, at least in qualitative terms. The framework establishes the basis on which further refinements can be made leading to the development of a robust decision making tool for filariasis control.

ACKNOWLEDGEMENTS

R. A. Norman acknowledges the support of the Carnegie Trust, D. A. P. Bundy acknowledges the support of the Wellcome Trust. M. S. Chan is a recipient of a Wellcome Trust Training Fellowship. E. Michael is in receipt of a MRC Fellowship. This study was supported by the Wellcome Trust.

REFERENCES

1. Michael E, Bundy DAP, Grenfell BT. Re-assessing the global prevalence and distribution of lymphatic filariasis. Parasitol 1996; **112**: 409–28.

2. Michael E, Bundy DAP. Global mapping of lymphatic filariasis. Parasitol Today 1997; **13**: 472–6.
3. Evans DB, Gelband H, Vlassoff C. Social and economic factors and the control of lymphatic filariasis: a review. Acta Trop 1993; **53**: 1–26.
4. Ramaiah KD, Guyatt H, Ramu K, Vanamail P, Pani SP, Das PK. Treatment costs and loss of work time to individuals with chronic lymphatic filariasis in rural communities in South India. Trop Med Int Health 1999; **4**: 19–25.
5. Ottesen EA, Ramachandran C. Lymphatic filariasis infection and disease: control strategies. Parasitol Today 1995; **11**: 129–31.
6. Ottesen EA, Duke BOL, Karam M, Behbehani K. Strategies and tools for the control/elimination of lymphatic filariasis. Bull WHO 1997; **75**: 491–503.
7. Anderson RM, May RM. Infectious diseases of humans: dynamics and control. Oxford: Oxford University Press, 1992: 489.
8. Hayashi SA. Mathematical analysis on the epidemiology of bancroftian filariasis and malayan filariasis in Japan. Jap J Exp Med 1962; **32**: 13–43.
9. Hairston NG, De Meillon B. On the inefficiency of transmission of *Wuchereria bancrofti* from mosquito to human host. Bull WHO 1968; **38**: 935–41.
10. Vanamail P, Subramanian S, Das PK, et al. Estimation of age specific rates of acquisition and loss of *Wuchereria bancrofti* infection. Trans R Soc Trop Med Hyg 1989; **83**: 689–93.
11. Bundy DAP, Grenfell BT, Rajagopalan PK. Immunoepidemiology of lymphatic filariasis: the relationship between infection and disease. Immunoparasitol Today 1991; **3**: A71–A75.
12. Grenfell BT, Michael E. Infection and disease in lymphatic filariasis: an epidemiological approach. Parasitol 1992; **104**: s81–s90.
13. Michael E, Bundy DAP. Herd immunity to filarial infection is a function of vector biting rate. Proc Roy Soc Series B 1998; **265**: 855–60.
14. Michael E. A different perspective on global mapping of lymphatic filariasis – Reply. Parasitol Today 1998; **14**: 333–4.
15. Pichon G, Perrault G, Laigret J. Rendement parasitaire chez les vecteurs de filarioses. Bull WHO 1974; **51**: 517–23.
16. Southgate BA, Bryan JH. Factors affecting transmission of *Wuchereria bancrofti* by anopheline mosquitoes 4. Facilitation, limitation, proportionality and their epidemiological significance. Trans Roy Soc Trop Med Hyg 1992; **86**: 523–30.
17. Plaisier AP, Subramanian S, Das PK, et al. The LYMFASIM simulation program for modeling lymphatic filariasis and its control. Meth Inform Med 1998; **37**: 97–108.
18. Chan MS, Srividya A, Norman RA, et al. Epifil: a dynamic model of infection and disease in lymphatic filariasis. Am J Trop Med Hyg 1998; **59**: 606–14.
19. Anderson RM, May RM. Helminth infections of humans – mathematical-models, population-dynamics, and control. Adv Parasitol 1985; **24**: 1–101.
20. Chan MS, Guyatt HL, Bundy DAP, Booth M, Fulford AJC, Medley GF. The development of an age structured model for schistosomiasis transmission dynamics and control and its validation for *Schistosoma mansoni*. Epidemiol Infect 1995; **115**: 325–44.
21. Dye C. Does facilitation imply a threshold for the eradication of lymphatic filariasis? Parasitol Today 1992; **8**: 109–10.
22. Subramanian S, Krishnamoorthy K, Ramaiah KD, Habbema JDF, Das PK, Plaisier AP. The relationship between microfilarial load in the human host and uptake and development of *Wuchereria bancrofti* microfilariae by *Culex quinquefasciatus*: a study under natural conditions. Parasitol 1998; **116**: 243–55.
23. Subramanian S, Pani SP, Das PK, Rajagopalan PK. Bancroftian filariasis in Pondicherry, South India: 2. Epidemiological evaluation of the effect of vector control. Epidemiol Infect 1989; **103**: 693–702.
24. Das PK, Manoharan A, Subramanian S, et al. Bancroftian filariasis in Pondicherry, South India – epidemiological impact of recovery of the vector population. Epidemiol Infect 1992; **108**: 483–93.
25. Rajagopalan PK, Das PK, Subramanian S, Vanamail P, Ramaiah KD. Bancroftian filariasis in Pondicherry, South India: 1. Pre-control epidemiological observations. Epidemiol Infect 1989; **103**: 685–92.
26. Dreyer G, Addiss D, Santos A, Figueredo-Silva J, Noroes J. Direct assessment *in vivo* of the efficacy of combined single dose ivermectin and diethylcarbamazine against adult *Wuchereria bancrofti*. Trans Roy Soc Trop Med Hyg 1998; **92**: 219–22.
27. Ramaiah KD, Das PK, Dhanda V. Estimation of permissible levels of transmission of bancroftian filariasis based on some entomological and parasitological results of a 5-year vector control programme. Acta Trop 1994; **56**: 89–96.
28. Michael E, Ramaiah KD, Hoti SL, et al. Quantifying mosquito biting patterns on humans by DNA fingerprinting of bloodmeals. Am J Trop Med Hyg. In press.
29. Ottesen EA. Infection and disease in lymphatic filariasis: an immunological perspective. Parasitol 1992; **104**: S71–S79.
30. Baldwin CI, Demedeiros F, Denham DA. Ige Responses in cats infected with *Brugia–Pahangi*. Parasite Immunol 1993; **15**: 291–6.
31. Weil GJ, Lammie PJ, Weiss N. The ICT filariasis test: A rapid-format antigen test for diagnosis of bancroftian filariasis. Parasitol Today 1997; **13**: 401–4.
32. Amaral F, Dreyer G, Figueredo-Silva J, et al. Live adult worms detected by ultrasonography in human bancroftian filariasis. Am J Trop Med Hyg 1994; **50**: 753–7.
33. Dreyer G, Amaral F, Noroes J, Medeiros Z. Ultrasonographic evidence for stability of adult worm location in bancroftian filariasis. Trans Roy Soc Trop Med Hyg 1994; **88**: 558.
34. Ismail MM, Jayakody RL, Weil GJ, et al. Efficacy of single dose combinations of albendazole, ivermectin

and diethylcarbamazine for the treatment of bancroftian filariasis. Trans Roy Soc Trop Med Hyg 1998; **92** : 94–7.
35. Rajagopalan PK. Population dynamics of *Culex pipiens fatigans*, the filariasis vector, in Pondicherry – influence of climate and environment. Proc Ind Nat Science Acad 1980; **B46**: 745–52.
36. Subra R. WHO/VBC/80.781.1980.
37. Subramanian S, Manoharan A, Ramaiah KD, Das PK. Rates of acquisition and loss of *Wuchereria bancrofti* infection in *Culex quinquefasciatus*. Am J Trop Med Hyg 1994; **51** : 244–9.
38. Ho BC, Ewert A. Experimental transmission of filarial larvae in relation to feeding behaviour of the mosquito vector. Trans Roy Soc Trop Med Hyg 1967; **61** : 663–6.
39. Ottesen EA. Efficacy of diethylcarbamazine in eradicating infection with lymphatic dwelling filariae in humans. Rev Infect Dis 1985; **7** : 341–56.
40. Vanamail P, Subramanian S, Das PK, Pani SP, Rajagopalan PK. Estimation of fecundic lifespan of *Wuchereria bancrofti* from longitudinal study of human infection in an endemic area of Pondicherry (South India). Ind J Med Res 1990; **91** : 293–7.
41. Vanamail P, Ramaiah KD, Pani SP, Das PK, Grenfell BT, Bundy DAP. Estimation of the fecund lifespan of *Wuchereria bancrofti* in an endemic area. Trans Roy Soc Trop Med Hyg 1996; **90** : 119–21.
42. Hairston NG, Jachowski LA. Analysis of the *Wuchereria bancrofti* population in the people of American Samoa. Bull WHO 1968; **38** : 29–59.